Table II
α-Helix Content $[\theta]_H$ of *P. c. ricini* Silk Fibroin in Aqueous Solution Determined with ^{13}C NMR and CD Methods as a Function of Temperature

temp, °C	mean helicity[a]	$[\theta]_H^{C=O}$ [b]	$[\theta]_H^{CO}$ [c]
-5	0.76	25.9	
0	0.76	25.9	
5	0.68	23.2	22.0[d]
10	0.62	21.1	
15	0.53	18.0	18.8
20			17.6
25	0.45	15.3	

[a] The helicity of the -$(Ala)_{22}$- sequence portion determined by both ^{13}C NMR and thermodynamic analyses (Figures 8 and 9). [b] Determined from the product of the α-helix fraction (h + h*; 0.341) and the mean helicity. [c] Determined from the CD method. [d] At 4 °C.

reported previously although the same NMR data are used. This is due to an assumption that the mean helicity of the alanine sequence at 0 °C is 100% in the previous paper. However, the mean helicity at 0 °C should be 76% when the number of the alanine residues of the sequence is 22 as mentioned above. Thus, it is necessary to know the number of alanine residues in estimating the α-helix content of *P. c. ricini* silk fibroin with the ^{13}C NMR method.

References and Notes

(1) Kuzuhara, A.; Asakura, T.; Tomoda, R.; Matsunaga, T. *J. Biotechnol.* **1986**, *5*, 199-207.
(2) Grasset, L.; Cordier, D.; Couturier, R.; Ville, A. *Biotechnol. Bioeng.* **1983**, *25*, 1423-1434.
(3) Asakura, T.; Yoshimizu, H.; Kuzuhara, A.; Matsunaga, T., submitted for publication in *J. Seric. Sci. Jpn.*
(4) Shimura, K. *Zoku Kenshi no Kozo (Structure of Silk Fibers)*; Hojo, N., Ed.; Shinshu University: Ueda, Japan, 1980.
(5) Asakura, T.; Suzuki, H.; Watanabe, Y. *Macromolecules* **1983**, *16*, 1024-1026.
(6) Saito, H.; Iwanaga, Y.; Tabeta, R.; Narita, M.; Asakura, T. *Chem. Lett.* **1983**, 427-430.
(7) Asakura, T.; Murakami, T. *Macromolecules* **1985**, *18*, 2614-2619.
(8) Asakura, T.; Suzuki, H.; Tanaka, T. *J. Seric. Sci. Jpn.* **1985**, *54*, 504-509.
(9) Asakura, T. Proceeding of the 7th International Wool Textile Research Conference, Tokyo, Sakamoto, M., Ed.; 1985; Vol. 1, pp 354-363.
(10) Bixon, M.; Scheraga, H. A.; Lifson, S. *Biopolymers* **1963**, *1*, 419-429.
(11) Kirimura, J. *Bull. Ser. Exp. Stn.* **1962**, *17*, 447-514.
(12) Iizuka, E. *Biochim. Biophys. Acta* **1968**, *160*, 454-463.
(13) Lifson, S.; Roig, A. *J. Chem. Phys.* **1961**, *34*, 1963-1974.
(14) Ullman, R. *Biopolymers* **1970**, *9*, 471-487.
(15) Platzer, K. E. B.; Ananthanarayanan, V. S.; Andreatta, R. H.; Scheraga, H. A. *Macromolecules* **1972**, *5*, 177-187.
(16) Matheson, R. R., Jr.; Scheraga, H. A. *Macromolecules* **1983**, *16*, 1037-1043.

Synthesis, NMR Characterization, and Electrical Properties of Siloxane-Based Polymer Electrolytes

R. Spindler and D. F. Shriver*

Northwestern University, Department of Chemistry, 2145 Sheridan Road, Evanston, Illinois 60201.

Received June 10, 1987

ABSTRACT: A cross-linked siloxane-based polymer has been prepared by the reaction of poly(methylhydrosiloxane), poly(ethylene glycol) monomethyl ether, and poly(ethylene glycol). The polymer, which has been structurally characterized by ^{29}Si NMR, forms complexes with $LiSO_3CF_3$ that exhibit good ionic conductivities (up to 7.3×10^{-5} Ω^{-1} cm^{-1}, 40 °C, for a $LiSO_3CF_3$ 15 wt % complex). The polymer and its salt complexes have been characterized by elemental analysis, ^{29}Si NMR, X-ray powder diffraction, DSC, and ac complex impedance spectroscopy. The dependence of the ionic conductivity was investigated as a function of temperature, salt concentration (1-25 wt %), and alkali-metal cation (Li, Na, K, Rb, and Cs).

Introduction

Solvent-free polymer electrolytes can be formed by the interaction of polar polymers with metal salts.[1,2] Ion transport in these electrolytes has been a topic of considerable research in the last 5 years, and this field has been recently reviewed.[3] The currently accepted model for ionic conductivity has led to the synthesis of network and comb polymers that have a high degree of segmental motion as judged by low values of the glass transition temperature, T_g.[4,5]

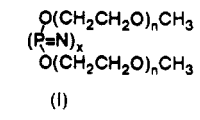

(I)

(II)

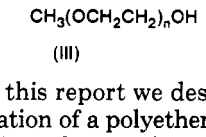

(III)

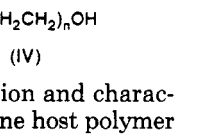

(IV)

In this report we describe the preparation and characterization of a polyether-substituted siloxane host polymer and its salt complexes. We were prompted to prepare these materials because siloxanes typically exhibit low values of T_g. The siloxane polymer was prepared from the reaction of poly(methylhydrosiloxane), PMHS (II); poly(ethylene glycol) monomethyl ether, MePEG(III); and poly(ethylene glycol), PEG (IV). Other groups have investigated siloxane-based electrolytes but in most cases the polymer was a block copolymer of dimethylsiloxane and ethylene oxide repeat units.[6] A urethane network formed from poly(dimethylsiloxane-*graft*-ethylene oxide) has also been studied.[7] While the work presented in this paper was in progress, other groups reported preliminary results on similar polymers and electrical measurements.[8]

Experimental Section

Poly(ethylene glycol) monomethyl ether, MePEG (Aldrich, MW_{av} = 350); poly(ethylene glycol), PEG (Aldrich, MW_{av} = 300); and poly(methylhydrosiloxane), PMHS (Petrarch, MW = 4500-5000), were dried under vacuum at 60 °C for 2 days, no evidence of H_2O in any of the starting materials was noted by IR spectroscopy. A zinc octoate catalyst (Petrarch, 50 wt % PDMS) was used as received. The polymer host that we designate as siloxane(30) was prepared by the reaction of a stoichiometric

0024-9297/88/2221-0648$01.50/0

amount of PMHS (2.00 g), MePEG (8.15 g), and PEG (1.50 g) and ca. 50 mg of zinc octoate/PDMS in xylene at 130 °C for ca. 4 h under a flow of Ar. The terminology siloxane(30) is used to indicate that if all the PEG were incorporated into cross-links and no other cross-links were present, 30% of the siloxane repeat units would be cross-linked. Of course, some of the PEG will double back to the same polymer chain and therefore not form a cross-link. Also, NMR data, described later, indicate that there are additional sources of cross-links in these materials. The mixture was then cooled to room temperature and the solvent was removed under vacuum. During the removal of solvent the reaction mixture was slowly reheated to 130 °C. After ca. 2 h at this temperature, a colorless solid formed. The solid was washed for 1–4 days with CH_2Cl_2 in a Soxhlet extractor to remove unreacted polyethers and the catalyst. Siloane(30) was dried under vacuum (ca. 2×10^{-5} Torr) for more than 48 h and stored in a dry, inert atmosphere. Elemental analysis gave a good correlation between the observed and desired composition: Anal. Found (calcd), C 47.28 (47.83), H 8.26 (8.46), and Si 7.50 (7.16). The undoped siloxane(30) had a conductivity of ca. 4×10^{-8} Ω^{-1} cm^{-1} (40 °C), which is 3 orders of magnitude lower than the conductivity of the salt complexes described here. The conductivity of the parent polymer probably arises from ionic impurities. A potential source for the impurities is residual catalyst.

The salts used in preparation of the complexes were either obtained from commercial sources, $LiSO_3CF_3$ and $NaSO_3CF_3$ (Alfa), or synthesized from the reaction of HSO_3CF_3 (Aldrich) with MOH, M = K, Rb, and Cs (Aldrich). In all cases the salts were recrystallized from CH_3CN/C_6H_6 and then dried under vacuum (100 °C, 2×10^{-5} Torr) for 2–4 days. The salts were stored in a dry, inert atmosphere. Salt complexes were prepared by weighing a stoichiometric quantity of salt and siloxane(30) in a dry, inert atmosphere. Acetonitrile (previously distilled from CaH_2) was added, and the solvent-swollen polymer was kept in contact with the solution for 1 day. Upon removal of the solvent, a separate salt phase was not present. The complexes were dried under vacuum at ca. 60 °C for 2 days and then stored in a dry, inert atmosphere. Throughout this paper, the concentrations of salt are reported as weight percentages, because the more conventional concentration units such as polymer repeat unit per salt formula unit are not well defined for these cross-linked systems. The homogeneous polymer–salt complex was analyzed for sulfur (in $SO_3CF_3^-$) and the results agreed with those calculated for the polymer to salt ratio employed in the preparation: Anal. Found (calcd) for siloxane(30) $LiSO_3CF_3$ 5%, 0.99 (1.03); for siloxane(30) $LiSO_3CF_3$ 10%, 2.05 (2.06); for siloxane(30) $LiSO_3CF_3$ 15%, 3.16 (3.08); and for siloxane(30) $LiSO_3CF_3$ 20%, 3.73 (4.11). As judged by X-ray powder diffraction, no crystalline salt was present in any of the polymer salt complexes.

The ^{29}Si NMR spectra were obtained on a Varian XL-400 spectrometer operating at 79.5 MHz. $Cr(acac)_3$, ca. 10 mM, was used as a spin relaxant and C_6D_6 was employed for the deuterium lock. NMR spectra of solid siloxane(30) were obtained on the xylene-swollen polymer Tetramethylsilane was used as an internal standard. All spectra were obtained at ambient temperatures with the spectral width set to 12 KHz, pulse width of 23 μs, and pulse delay time of 5 s, and a line broadening of 4 Hz was employed.

DSC traces were obtained on a Perkin-Elmer DSC-2 equipped with liquid-nitrogen cooling. Values of T_g were determined at the midpoint of the inflection. Cold crystallization exotherms and melting endotherms were measured at the peak of the transition. The temperature scale was calibrated by using five standards (In, naphthalene, Ga, Hg, and heptane). All transitions were obtained at three heating rates (usually 80, 40, and 20 deg/min) and the reported transitions were found by extrapolating to a 0 deg/min heating rate. X-ray powder diffraction traces were obtained on a Rigaku automated powder diffractometer, at room temperature, using Cu Kα radiation.

Samples for ac impedance analysis were pressed into pellets inside air-tight conductivity cells. The manipulation of all samples was performed under a dry, inert, and nitrogen-free atmosphere. Pt (Goldsmith) or Li (ribbon, Foote Mineral Co.) electrodes were used in these measurements. The surface area of the electrodes was 1.27 cm^2 and the sample length varied from 0.05 to 0.1 cm. The frequency-dependent impedance of the samples was measured on a HP 4192A impedance analyzer (5 MHz to 5 Hz) or a Solartron 1250 frequency response analyzer/1286 potentiostat ystem (1 KHz to 10^{-3} Hz). Good agreement was found in the region where data from the two different instruments overlap. The sample cell was placed in a regulated air bath (±0.1 K) for the temperature-dependent conductivity measurements. In the temperature range from 30 to −5 °C, CO_2(s) was placed in the oven cavity to maintain the temperature. The −23 °C data were obtained by placing the sealed conductivity cell in a CCl_4 slush bath. The temperature-dependent conductivity was fit to the VTF equation, eq 8, by a linear least-squares program where the parameter T_0 was varied until the best fit was obtained as judged by $\chi^2 = \sum(1/D_i)^2(\sigma_i^{calcd} - \sigma_i^{exptl})^2$. D_i is the deviation in the experimental conductivity data, σ_i^{calcd} is the calculated value of the conductivity, eq 8, and σ_i^{exptl} is the experimental value of the conductivity. The best fit was obtained when $\chi^2 = 1$.

Results and Discussion

Synthesis and Characterization of the Polymer Host. Equation 1 shows the general reaction used to prepare a polyether-substituted siloxane polymer. A study

$$(SiH(CH_3)O)_x + ROH \xrightarrow{\text{catalyst}} (Si(OR)(CH_3)O)_x + H_2(g) \quad (1)$$

of the literature reveals that a wide variety of catalyst have been employed to promote the reaction of silanes with alcohol, including $ZnCl_2$, $SnCl_2$, NEt_3, and Na_2CO_3.[9] Zinc dioctoate is used here as it is soluble in organic solvents. Scheme I summarizes the procedure used in the polymer preparation. A stoichiometric mixture of PMHS, MePEG,

Scheme I

$$\text{PMHS} + (a/2)\text{PEG} + (1-a)\text{MePEG} \xrightarrow[130\ ^\circ\text{C},\ 4\ \text{h}]{\text{xylene}} \xrightarrow[130\ ^\circ\text{C},\ 2\ \text{h}]{\text{vacuum}} \xrightarrow[CH_2Cl_2]{\text{Soxhlet}} \xrightarrow[60\ ^\circ\text{C},\ 48\ \text{h}]{\text{vacuum}} \text{siloxane(30)}$$

and PEG were allowed to react together in xylene. PEG was employed as a cross-linking reagent, since the commercially available PMHS is a viscous liquid of ca. 5000 MW. A cross-linking density of 30% ($a = 0.3$) was found to give the best combination of high ionic conductivity and good mechanical properties.

^{29}Si NMR was an excellent probe of the structure of siloxane(30), because of the wide chemical shift range, distinctive chemical shift values, and availability of extensive chemical shift information for both molecular[10] and polymeric systems.[11] Figure 1 shows the ^{29}Si NMR spectrum of solid siloxane(30) after impurities had been extracted from it with CH_2Cl_2 and volatiles removed under vacuum. Three signals are observed at −49.8, −57.8, and −65 ppm as well as a very broad resonance centered at ca. −115 ppm, which is due to the glass NMR tube. By comparison with NMR data for both molecular silanes[10] and polymeric siloxanes[11] we can assign the peaks as follows: $M^{(OR)_2}$ (−49.8 ppm), D^{OR} (−57.8 ppm), and T (−65 ppm). The notation used here is explained in Figure 1. The reaction appears to have gone to completion as judged by the absence of signals due to free SiH (D^H, −33.8 ppm) moieties. Attempts to limit the formation of $M^{(OR)_2}$ and T groups by lowering the reaction temperature, decreasing the concentration of the catalyst, or changing the catalyst from zinc dioctoate to $ZnCl_2$, $SnCl_2$, and K_2CO_3 had only a slight effect on the product distribution. Addition of up to 5% H_2O (based on PMHS) to the reaction mixture resulted in no significant change in the observed products. The synthetic procedure of Smid and co-workers[8b] was also employed, but the spectrum for the product indicated a distribution of structures similar to that found for our original product.

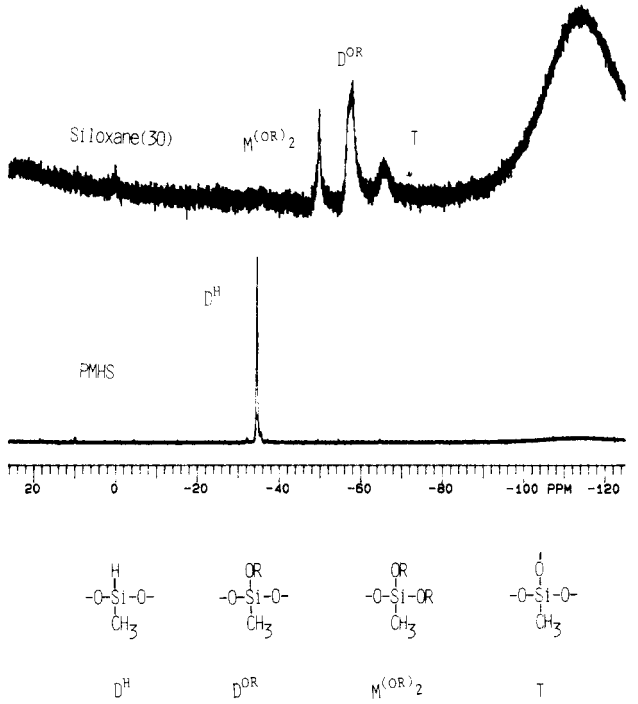

Figure 1. ^{29}Si NMR spectrum of solvent swollen siloxane(30) (top spectrum) and poly(methylhydrosiloxane) (lower spectrum). The broad resonance on the right-hand side of the siloxane(30) spectrum is due to the glass of the NMR tube. The siloxane nomenclature used in this paper is shown at the bottom of this figure.

A mechanism for the formation of siloxane(30) is proposed in eq 2–6. We believe that the formation of the

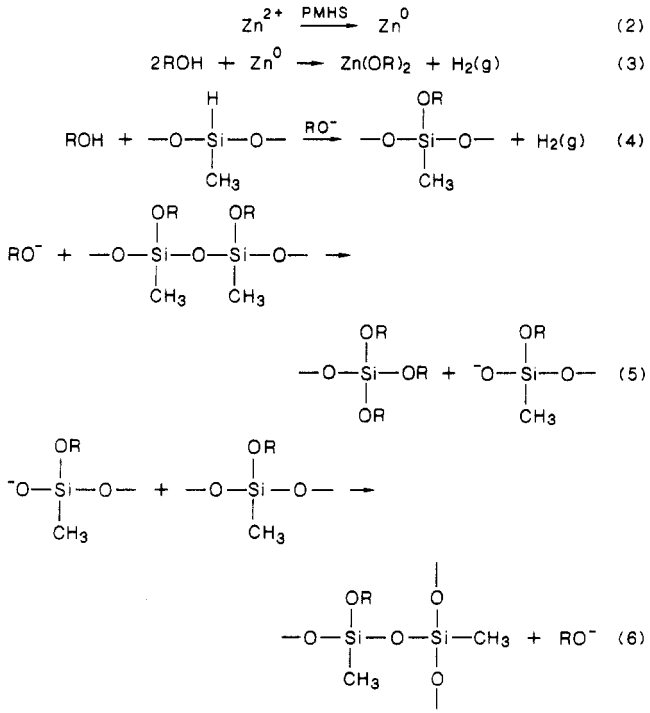

monoalkoxy-substituted siloxane moiety (D^{OR}) is catalyzed by an alkoxide, eq 4. The preparation of alkoxy-substituted silanes has been carefully studied[12] and a number of workers have shown that the alkoxide attacks the silane center in a S_N2 fashion to liberate the hybride, eq 7. The hydride is not a good leaving group but its displacement

$$HSiR_3 + R'OH \xrightarrow{R'O^-} R'OSiR_3 + H_2(g) \quad (7)$$

Table I
DSC Data for Siloxane(30) and Its Salt Complexes

polymer	T_g, K ± 2 K	T_{cc}, K ± 3 K	T_m, K ± 3 K
PMHS	133		
PEG	191	213	255
MePEG	178	205, 221	246, 266
siloxane(30)	204	218	264
siloxane(30) $LiSO_3CF_3$ 1%	204	220	261
siloxane(30) $LiSO_3CF_3$ 2.5%	207	217	263
siloxane(30) $LiSO_3CF_3$ 5.0%[a]	210	230	264
siloxane(30) $LiSO_3CF_3$ 7.5%	213		
siloxane(30) $LiSO_3CF_3$ 10%	215		
siloxane(30) $LiSO_3CF_3$ 12.5%	219		
siloxane(30) $LiSO_3CF_3$ (15.0%	220		
siloxane(30) $LiSO_3CF_3$ 17.5%	226		
siloxane(30) $LiSO_3CF_3$ 20.0%	231		
siloxane(30) $LiSO_3CF_3$ 25.0%	235		
siloxane(30) $NaSO_3CF_3$ 5.5%[a]	209	230	258
siloxane(30) KSO_3CF_3 6.0%[a]	206	232	259
siloxane(30) $RbSO_3CF_3$ 7.5%[a]	206	225	257
siloxane(30) $CsSO_3CF_3$ 9.0%[a]	206	232	257

[a] These complexes all contain the same number of moles of cations to moles of polymer repeat units.

is assisted by reacting with a proton from the alcohol to form $H_2(g)$. This last step regenerates the catalytic alkoxide. In the synthesis of siloxane(30), the alkoxide catalyst is formed in two steps, eq 2 and 3. First Zn^{2+} is reduced by PMHS to finely divided zinc metal which is then followed by the reaction of the polyethers with Zn^0 to form the alkoxide. The reduction of Zn^{2+} to Zn^0 is reasonable as PMHS is known to be a fairly strong reducing agent.[13] Even more compelling evidence for this interpretation is the observation that if insufficient polyether is used during the synthesis of siloxane(30), zinc metal is observed to form. The formation of the $M^{(OR)_2}$ and T moieties appears to be associated with the presence of base, eq 5 and 6. The effect of base on the Si–O–Si linkage has been well documented.[14] An example of this reaction is shown in eq 8 where base cleaves the Si–O–Si bond in disiloxane to form siloxides.[15] Also basic catalysts

$$[(CH_3)_3Si]_2O + 2NaOH \rightleftharpoons 2(CH_3)_3SiONa + H_2O \quad (8)$$

are important in the ring-opening polymerization of cyclic siloxanes to produce linear siloxane polymers.[16] In the synthesis of siloxane(30), the alkoxide breaks the Si–O–Si bond to give the $M^{(OR)_2}$ moiety and a siloxide, eq 5. The siloxide can then react with a D^{OR} group to form the T moiety as is shown in eq 6. A similar reaction has been used to prepare a monomeric analogue of the T groups, eq 9.[17] Siloxane(30) and its salt complexes have also been

$$4(CH_3)SiOH + (EtO)_3SiCH_3 \xrightarrow{NaOSi(CH_3)_3} [(CH_3)_3SiO]_3SiCH_3 + 4EtOH \quad (9)$$

characterized by solid-state ^{13}C NMR spectroscopy and this work will be described in another paper.[18]

Characterization of the Polymer Salt Complexes. The thermal properties of siloxane(30) and its salt complexes, which were investigated by differential scanning calorimetry (DSC), are listed in Table I. A single glass transition temperature was observed at 204 K in DSC scans for siloxane(30), which were conducted over the temperature range 110–400 K. As siloxane(30) is heated past T_g, an exothermic cold crystallization is observed followed by an endothermic melting transition. The cold crystallization is observed when the sample is quenched at rates greater than 10 deg/min, as the sample forms a metastable glassy state. At slower cooling rates the polymer crystallizes and the exothermic transition is not

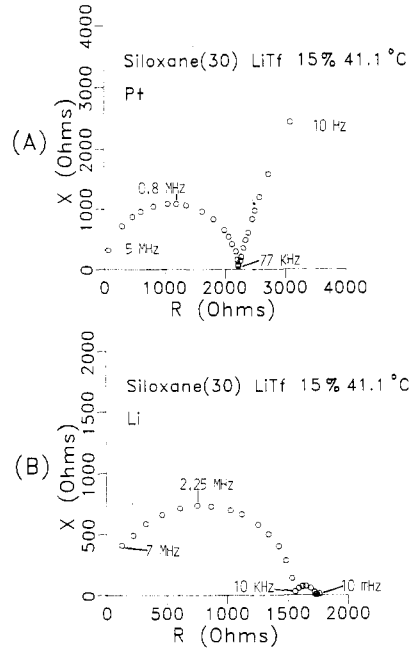

Figure 2. Complex impedance spectra of siloxane(30) $LiSO_3CF_3$ 15% with ion-blocking Pt electrodes (A) and cation reversible Li electrodes (B). The different scales on the two plots are due to the different geometric factors of the polymer electrolytes used in these two experiments.

seen. The similarity of the cold crystllization and melting temperatures between siloxane(30), MePEG, and PEG leads us to suggest that the polyether side groups crystallize but the siloxane backbone does not. The selective crystallization of side groups has been observed for other comb polymers.[19]

The presence of salt affects the ability of siloxane(30) to form an ordered crystalline phase. At salt concentrations greater than 5 wt % $LiSO_3CF_3$ (O:Li = 53:1), no crystalline phases are observed. Other alkali-metal salts influence T_g but not the cold crystallization or melting transitions (Table I). Ion–dipole interactions reduce the mobility of the polyether side chains, and therefore, T_g increases as the concentration of salt increases.

Impedance measurements on the polymer–salt complexes were acquired as a function of frequency (5 MHz to 10^{-3} Hz) in order to separate response of the bulk polymer electrolyte from polarization at the electrode.[20] Figure 2A shows a characteristic complex impedance plot for the siloxane(30) LiTf 15% complex sandwiched between ion-blocking Pt electrodes. The high-frequency semicircle is associated with the bulk properties of the polymer electrolyte. The low-frequency spur in the impedance plot arises from double-layer capacitance at the electrode–electrolyte interface. This assignment is confirmed by data obtained with cation-reversible lithium electrodes which yield impedance spectra which contain the high-frequency semicircle but have a small semicircle in place of the low-frequency spur, Figure 2B. The low-frequency semicircle is attributed to resistance and capacitance associated with the transfer of lithium cations between the electrolyte and the electrode. The stability of siloxane(30) electrolytes toward Li electrodes was qualitatively investigated by complex impedance measurements. At a given temperature no changes were noted in the impedance spectra when the sample was cycled between 40 and 80 °C over a 2-day period. Since the electrical properties of the lithium–polymer interface do not change, we assume that decomposition of the electrolyte is not occurring at the interface under these conditions. Hall and co-workers[8a] report that their "comblike" siloxane electrolyte is not stable to Li electrodes. Smid and co-workers[8b] did not report the stability of their electrolyte to lithium electrodes. It is our impression that many reports of polymer electrolyte instability toward lithium may actually originate from the reaction of impurities such as moisture, oxygen, or nitrogen with the lithium electrode.

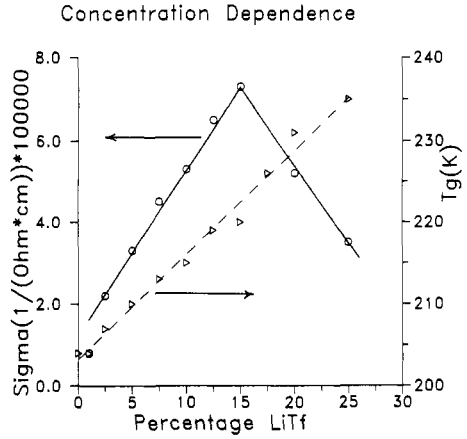

Figure 3. Concentration dependence of the ionic conductivity (left-hand axis, circles) and T_g (right-hand axis, triangles) for the siloxane(30) $LiSO_3CF_3$ salt complexes at 40 °C.

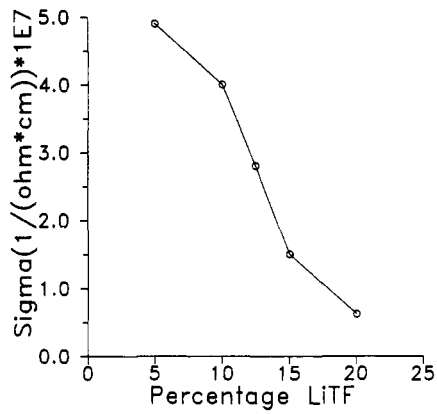

Figure 4. Conductivity of the siloxane(30) $LiSO_3CF_3$ polymer salt complexes as a function of salt concentration at −23 °C.

The effect of salt concentration on ionic conductivity can be broken down into two temperature regions. For the conductivity data collected in the temperature range 10–80 °C, a maximum in the conductivity is observed at 15% $LiSO_3CF_3$ (O:Li = 16.1), Figure 3. Similar behavior has been observed for both semicrystalline[4a,21] and amorphous polymer electrolytes.[5,22-24] At temperatures below 10 °C the maximum in the conductivity is shifted to lower salt concentrations as is shown in Figure 4 for the data collected at −23 °C. To aid our understanding of the concentration dependence of the ionic conductivity, we employ eq 10, which relates the conductivity (σ) to the concentration of charge carriers (n_i), the charge of the carriers (q_i), and their ionic mobility (μ_i). As the concentration

$$\sigma = \sum n_i q_i \mu_i \tag{10}$$

of salt in the electrolyte is increased, the number of charge carriers should also increase, although the increase in charge carriers may not be a linear function of salt concentration if ion pair or multiplet formation is significant. According to the excess entropy model,[25] ionic mobility is strongly influenced by T_g. Therefore it is instructive to look for an explanation of the maximum in the conduc-

Table II
VTF and Arrhenius Parameters

sample	A^a	B, eV[a]	T_0, K[a]	$T_g - T_0$, K	E, eV[b]
siloxane(30) $LiSO_3CF_3$ 2.5%	0.045	0.062	166	41	0.29
siloxane(30) $LiSO_3CF_3$ 5.0%	0.20	0.068	172	38	0.32
siloxane(30) $LiSO_3CF_3$ 10.0%	0.33	0.072	173	42	0.37
siloxane(30) $LiSO_3CF_3$ 15.0%	0.93	0.075	182	38	0.42
siloxane(30) $LiSO_3CF_3$ 20.0%	1.1	0.81	182	49	0.48

[a] Equation 11. [b] Equation 12.

tivity in terms of variations in T_g as has been discussed by previous workers.[5a,26]

Figure 3 shows that T_g increases in a linear fashion with a slope of 1.3 K/wt % $LiSO_3CF_3$. For data collected in the temperature range 10–80 °C the conductivity increases with increasing salt concentration up to 15 wt % $LiSO_3CF_3$, apparently due to an increase in the number of charge carriers. As the $LiSO_3CF_3$ concentration increases beyond 15%, the conductivity decreases. This decrease in conductivity can be explained by the excess entropy model for ion transport, eq 11. The T_0 term in that expression is closely related to T_g. As T_g increases T_0 also increases which lowers the ionic conductivity for polymer salt complexes that contain greater than 15% $LiSO_3CF_3$. Interestingly, the linear polyether-substituted phosphazene electrolytes exhibit a maximum in the conductivity at approximately the same ratio of ether oxygens to formula units of $LiSO_3CF_3$ (16:1) as found in the siloxane(30) salt complexes.[22] Even though the molecular structure of the siloxane(30) electrolyte is more complex than those of the phosphazene-based electrolytes, the concentration dependence, temperature dependence, and magnitude of the conductivity are comparable for the two electrolytes. The liquid electrolyte prepared by Smid and co-workers[8b] exhibits a maximum in the conductivity at an ether oxygen to lithium cation ratio of 25:1.

As we have previously stated, when the ionic conductivity is measured at lower temperatures the maximum in the conductivity shifts to lower salt concentrations for the $LiSO_3CF_3$–siloxane(30) system, Figure 4. For example, at −23 °C the maximum is observed at 5% $LiSO_3CF_3$. The basis for this shift is apparent in eq 8 because of the closer proximity of T to T_0 when the conductivity is measured at reduced temperatures.

In addition to the influence of polymer segmental motion on conductivity, ion–ion interactions may influence the concentration-dependence of the ionic conductivity. The concentration of charge carriers in a low dielectric medium such as polymer electrolytes is probably strongly influenced by the formation of ion pairs and multiplet ions. In the concentration range of salts used in the present studies (ca. 0.1–2 M), a significant degree of ion pair formation has been found in low dielectric constant solvents.[27] Also evidence for ion-pair formation has been obtained by Raman spectroscopy for PEO–$LiNO_3$ complexes,[28] and multiplet ion formation has been inferred for polyurethane salt complexes.[26] Recent work on low molecular weight polyethers has shown that the conducting species in polymer electrolytes are mot likely triplets and other higher order aggregates.[29] Further work needs to be done to probe the significance of ion-pair formation on conductivity in polymer electrolytes.

The temperature dependence of the ionic conductivity is shown in Figure 5 for siloxane(30) $LiSO_3CF_3$ 15% and siloxane(30) $LiSO_3CF_3$ 5%. For both complexes the plots are curved over the temperature range studied (80 to −23 °C). Curved log (σ) versus $1000/T$ plots are characteristic of amorphous electrolytes,[23a,27] although linear or close to linear plots are also observed.[22] The Vogel–Tamman–

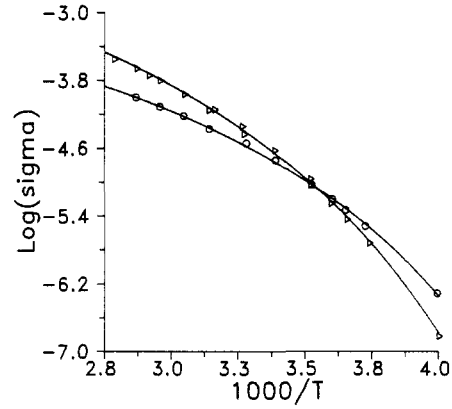

Figure 5. Temperature dependence of the ionic conductivity for siloxane(30) $LiSO_3C_3$ 5% (circles) and siloxane(30) $LiSO_3CF_3$ 15% (stars). The lines drawn through the data points were calculated from the best-fit parameters obtained from the VTF equation (eq 11) for each complex; see Table II for the parameters.

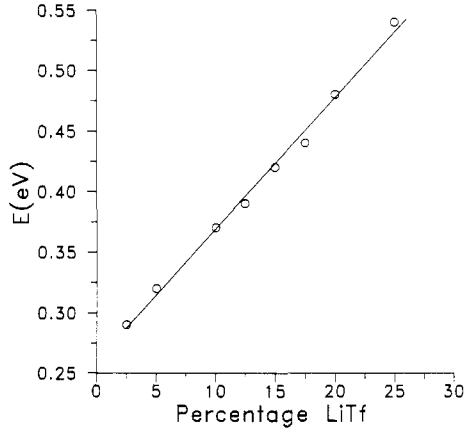

Figure 6. Arrhenius activation energies for siloxane(30) $LiSO_3CF_3$ salt complexes shown as a function of $LiSO_3CF_3$ contained in the electrolyte.

Fulcher (VTF) equation, eq 8, has been used to model the temperature-dependent conductivity of amorphous polymer electrolytes.[6b,23a,27] Both configurational entropy[25] and

$$\sigma = AT^{-1/2}e^{(-B/T-T_0)} \quad (11)$$

free volume[30] models have been used to derive the VTF equation. The significant parameters are B, the apparent activation energy, and T_0, a parameter that is normally found to be 30–60 °C below T_g. Table II lists the values of T_0 and B obtained by fitting eq 11 to the temperature-dependent conductivity data obtained for the siloxane(30) salt complexes. The preexponential factor, apparent activation energy, and T_0 all increase as the concentration of salt in the polymer increases. The T_0 values were found to be 40–50 °C below T_g. The nearly linear nature of the log (σ) versus $1000/T$ plot over the temperature range of 10–80 °C permits the use of the Arrhenius equation, eq 12, to determine activation energies.

$$\sigma = AT^{-1}e^{-(E/RT)} \quad (12)$$

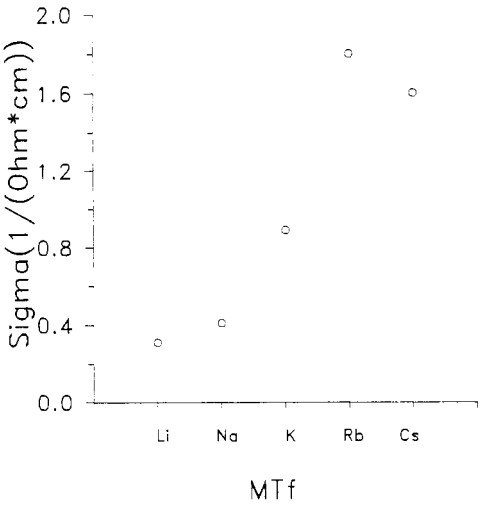

Figure 7. Ionic conductivity as a funtion of alkali-metal cation for the siloxane(30) MSO_3CF_3 (M = Li, Na, K, Rb, and Cs) complexes. Equimolar concentrations of salt were employed in these meausurements. The ionic conductivity was measured at 40 °C.

These activation energies are listed in Table II, and Figure 6 shows a plot of E versus the concentration of LiTf. The activation energies increase linearly as a function of concentration, which mirrors the behavior of T_g, Figure 3. The result suggests that T_g and the activation energy for charge transport are correlated.

Figure 7 exhibits the cation dependence of ionic conductivity for the alkali-metal trifluoromethane sulfonate salts (MSO_3CF_3; M = Li, Na, K, Rb, and Cs). In these experiments the concentration of MSO_3CF_3 was constant for each complex and equivalent to the concentration of MSO_3CF_3 found in siloxane(30) $LiSO_3CF_3$ 5%. All the values of T_g for the siloxane(30) MSO_3CF_3 complexes are within 3 K of one another so T_g should not appreciably influence the conductivity values we discuss in this section. The trend observed here is that conductivity increases with increasing radius of the cation from Li through Rb. Similar behavior has previously been observed in both aqueous and nonaqueous solution electrolytes[31] and also in poly(propylene oxide) network complexes with MSCN (M = Li, Na, and K).[32] The correlation between ionic radius and conductivity does not hold for $CsSO_3CF_3$ which has a lower total ionic conductivity than the $RbSO_3CF_3$ complex. In nonaqueous electrolytes size limitations on ionic mobilities have only been found for the larger NR_4^+ (R = alkyl) cations,[33] but for polymer electrolytes, the more constrained nature of the solvent may hinder the mobility of the larger Cs^+ cation.

Conclusions

A cross-linked polymer electrolyte based on a siloxane backbone has been synthesized. NMR data indicate that the structure of this polymer, siloxane(30), is complicated by the presence of Si–O–Si cross-links as well as the intended polyether cross-links. The electrolytes formed by incorporating alkali-metal salts into siloxane(30) display ionic conductivity that is as good as those observed for the structurally simpler polyphosphazene electrolytes. These results suggest that the high density of flexible cross-links in siloxane(30) does not significantly reduce segmental polymer motion. The cation dependence of the ionic conductivity for the siloxane(30) polymer electrolytes is similar to that for solution electrolytes.

Acknowledgment. L. C. Hardy performed the initial experiments in the synthesis of the siloxane electrolytes. The synthetic portion of this research was supported by a grant from the Office of Naval Research, N0014-80-C-0532; electrical measurements were performed under a grant from the Department of Energy, DE-FG02-85ER45220.

References and Notes

(1) Fenton, D. E.; Parker, J. M.; Wright, P. Y. *Polymer* **1973**, *14*, 589.
(2) Armand, M. B. *Solid State Ionics* **1983**, *9*, *10*, 745–754.
(3) (a) Armand, M. B. *Annu. Rev. Mater. Sci.* **1986**, *16*, 245–261. (b) MacCallum, J. R.; Vincent, C. A. *Polymer Electrolyte Reviews*; Elsevier: London, 1987. (c) Ratner, M. A.; Shriver, D. F. *Chem. Rev.*, in press.
(4) Killis, A.; LeNest, J.-F.; Cheradame, H.; Gandini, A. *Makromol. Chem.* **1982**, *183*, 2835–2846.
(5) (a) Blonsky, P. M.; Shriver, D. F.; Austin, P. E.; Allcock, H. R. *J. Am. Chem. Soc.* **1984**, *106*, 6854–6855. (b) Blonsky, P. M.; Shriver, D. F.; Austin, P. E.; Allcock, H. R. *Solid State Ionics* **1986**, *18*, *19*, 258–264. (c) Tonge, J. S.; Shriver, D. F. *J. Electrochem. Soc.* **1987**, *134*, 269–270.
(6) (a) Nagaoka, K.; Naruse, H.; Shinohara, I.; Watanabe, M. J. *Polym. Sci., Polym. Lett.* **1984**, *22*, 659–663. (b) Adamic, K. J.; Greenbaum, S. G.; Wintersgill, M.; Fontanella, J. J. *J. Appl. Phys.* **1986**, *60*, 1342–1345.
(7) Bouridah, A.; Dalard, F.; Deroo, D.; Cheradame, H.; LeNest, J. F. *Solid State Ionics* **1985**, *15*, 233–240.
(8) (a) Hall, P. G.; Davies, G. R.; McIntyre, J. E.; Ward, I. E.; Bannister, D. J.; LeBrocq, K. M. F. *Polym. Commun.* **1986**, *27*, 98–100. (b) Fish, D.; Khan, D. M.; Smid, J. *J. Polym. Prepr.* **1986**, *27*, 325–326.
(9) (a) Kohama, S.; Umeki, Y. *J. Appl. Polym. Sci.* **1977**, *21*, 863–867. (b) Dolgov, B. N.; Kharitonov, N. P.; Glushkova, N. E.; Khudobin, I. I. *J. Gen. Chem. USSR* **1959**, *28*, 2737–2740.
(10) (a) Levy, G. C.; Cargioli, J. D. In *NMR of Nuclei Other than Protons*; Axenrod, T., Webb, G. A., Eds.; Wiley-Interscience: New York, 1970; pp 251–274. (b) Williams, E. A.; Cargioli, J. D. In *Annual Reports on NMR Spectroscopy*; Webb, G. A., Ed.; Academic: New York, 1979; Vol. 9, pp 221–318.
(11) (a) Harris, R. K.; Kennedy, J. D.; McFarlane, W. In *NMR and the Periodic Table*; Harris, R. K., Mann, B. E., Eds.; Academic: New York, 1978; pp 309–377. (b) Beshah, K.; Mark, J. E.; Ackerman, J. L.; Himstedt, A. *J. Polym. Sci., Polym. Phys. Ed.* **1986**, *24*, 1207–1225.
(12) (a) Sternbach, B.; MacDiarmid, A. G. *J. Am. Chem. Soc.* **1959**, *81*, 5109–5110. (b) O'Donnel, K.; Bacon, R.; Chellappa, K. L.; Schowen, R. L.; Lee, J. K. *J. Am. Chem. Soc.* **1972**, *94*, 2500–2505. (c) Eaborn, C.; Jenkins, I. D. *J. Organomet. Chem.* **1974**, *69*, 185–192.
(13) (a) Scott, W. J.; Stille, J. K. *J. Am. Chem. Soc.* **1986**, *108*, 3033–3040. (b) Keiman, E.; Greenspoon, N. *J. Org. Chem.* **1983**, 48, 3545–3548. (c) Lipowitz, J.; Bowman, S. A. *J. Org. Chem.* **1973**, *38*, 162–165.
(14) Bayant, V.; Chvalovsky, V. *Chemistry of Organosilicon Compounds*; Academic: New York, 1965; Vol. 1, pp 47–50.
(15) Hyde, j. F.; Johannson, O. K.; Daudt, W. H.; Flemming, R. F.; Laudenslager, H. B.; Roche, M. P. *J. Am. Chem. Soc.* **1953**, *75*, 5615–5618.
(16) Sowmani, P. M.; Minton, R. J.; McGrath, J. E. In *Ring-Opening Polymerization*; McGrath, J. E., Ed.; ACS Symposium Series 286; American Chemical Society: Washington, DC, 1985; pp 147–160.
(17) Sommer, L. H.; Green, L. Q.; Whitmore, F. C. *J. Am. Chem. Soc.* **1949**, *71*, 3253–3254.
(18) Spindler, R.; Shriver, D. F. *J. Am. Chem. Soc.*, in press.
(19) Wunderlich, B. *Macromolecular Physics*; Academic: New York, 1980; Vol. 3, pp 315–331.
(20) Macdonald, J. R. *J. Chem. Phys.* **1974**, *61*, 3977–3996.
(21) Dupon, R.; Papke, B. L.; Ratner, M. A.; Shriver, D. F. *J. Electrochem. Soc.* **1984**, *131*, 586–589.
(22) Tonge, J. S.; Blonsky, P. M.; Shriver, D. F.; Allcock, H. R.; Austin, P. E.; Neenan, T. X.; Sisko, J. T. *Extended Abstracts*; 170th National Meeting of the Electrochemical Society, 1986.
(23) (a) Armand, M. B.; Chabagno, J. M.; Duclot, M. J. In *Fast Ion Transport in Solids. Electrodes and Electrolytes*; Vashista, P., Mandy, J. N., Shenoy, G. K., Eds.; North-Holland: New York, 1979; pp 131–136. (b) Watanabe, M.; Sanui, K.; Ogata, N.; Inone, F.; Kobayashi, T.; Ohtaki, Z. *Polym. J.* **1985**, *17*, 549–555.
(24) (a) Cheradame, H.; Souquet, J. L.; Latour, J. M. *Mater. Res. Bull.* **1980**, *15*, 1173–1177. (b) Kobayashi, N.; Ychiyama, M.; Shigehara, K.; Tsuchida, E. *J. Chem. Phys.* **1985**, *84*, 987–991.

(25) Gibbs, J. H.; Adam, G. J. *J. Chem. Phys.* **1965**, *43*, 139-146.
(26) Cheradame, H. In *IUPAC Macromolecules*; Benoit, H., Rempp, P., Eds.; Pergamon: New York, 1982; pp 251-264.
(27) (a) Marcus, Y. *Ion Solvation*; Wiley: New York, 1985; pp 180-184. (b) Davies, C. W. *Ion Association*; Butterworths: Washington, 1962; pp 150-161. (c) Irish, D. E. In *Physical Chemistry of Organic Solvent Systems*; Covington, A. K., Dickinson, T., Eds.; Plenum: New York, 1973; pp 433-460.
(28) Papke, B. L.; Ratner, M. A.; Shriver, D. F. *J. Electrochem. Soc.* **1982**, *129*, 1434-1438.
(29) MacCallum, J. R.; Tomlin, A. S.; Vincent, C. A. *Eur. Polym. J.* **1986**, *22*, 787-791.
(30) Turnbill, D.; Cohen, M. H. *J. Chem. Phys.* **1970**, *52*, 3038-3041.
(31) Spiro, M. In *Physical Methods of Chemistry*; Rossiter, B. W., Hamilton, J. E., Eds.; Wiley: New York, 1986; Vol. 2, pp 663-791.
(32) Watanabe, M.; Sanui, K.; Ogata, N.; Inouye, F.; Kobayashi, T.; Ohtiki, Z. *Polym. J.* **1985**, *17*, 549-555.
(33) Jansen, M. L.; Yeager, H. L. *J. Phys. Chem.* **1973**, *26*, 3089-3092.

Phase Relationships and Conductivity of the Polymer Electrolytes Poly(ethylene oxide)/Lithium Tetrafluoroborate and Poly(ethylene oxide)/Lithium Trifluoromethanesulfonate

S. M. Zahurak,* M. L. Kaplan, E. A. Rietman, D. W. Murphy, and R. J. Cava

AT&T Bell Laboratories, Murray Hill, New Jersey 07974. *Received July 8, 1987*

ABSTRACT: Solid polymer electrolytes are potentially useful in all solid-state rechargeable batteries because of their elastic properties that allow for reduced interfacial contact resistance between the electrolyte and electrodes as well as for thin-film configurations. In this work a study of the complexes of poly(ethylene oxide) with two different salts, $LiBF_4$ and $LiCF_3SO_3$, is presented. As a result pseudobinary pseudoequilibrium phase diagrams (PPD) have been constructed that provide an improved basis for understanding the mechanism of ionic transport. Differential scanning calorimetry and X-ray diffraction have been used to collect data necessary for the PPD. A single-phase crystalline complex over the stoichiometries between 4:1 (monomer/salt) and 3:1 has been established in the case of the BF_4 salt. The $PEO_8(LiBF_4)$ sample exhibited the highest conductivity (9×10^{-4} S/cm) with an activation energy of 0.27 eV. The $LiCF_3SO_3$ complex was unusual in that evidence for a second complex (7:1) was obtained in addition to the more commonly observed 3.5:1 phase. These results were compared to phase diagrams published by others for the same and similar systems.

Since the discovery of fast alkali ion conductivity in polymer salt complexes (conductivity $>10^{-5}$ S/cm at 80 °C)[1] researchers have been avidly seeking a solid polymeric electrolyte (SPE) that would solve the chemical reactivity problems of lithium anodes with the more commonly used liquid organic and solid electrolytes in batteries. Two simple polymer systems have been studied most extensively, poly(ethylene oxide) [PEO] and poly(propylene oxide) [PPO]. A large number of complexes are formed by these polymers, a list of some of them has been compiled by Armand and co-workers.[2]

Despite studies by many groups, most of which have concentrated on complexes of PEO with salts such as $LiClO_4$ and $LiCF_3SO_3$, the structure and conductivity mechanism remain unclear. This study presents pseudobinary pseudoequilibrium phase diagrams (PPD) that furnish important compositional information and lay the structural groundwork which is crucial for understanding the conductivity processes. The polymer/salt systems cannot be described as true binary systems as in typical alloy phase diagrams because both the polymer (PEO) and the polymer/salt complex each contain crystalline and amorphous phases. In addition, these phases are present in variable amounts depending on temperature which means they are not necessarily at an equilibrium state. Therefore, these diagrams are referred to as pseudophase diagrams (PPD). These data concentrate on two PEO/Li^+ systems and compare conductivity results with PPD information. A comparison is also made between this work and similar efforts by Minier, Berthier, and co-workers, which stresses NMR results.[3] Pseudo phase diagram information has been compiled through differential scanning calorimetry and X-ray diffraction. The $PEO/LiBF_4$ system was chosen as the subject of study for its good total conductivity as found in a survey study of Li^+ conductors at moderate temperatures (10^{-5} S/cm at 60 °C).[4] The other system included here, and on which the majority of studies to date has concentrated, is $PEO/LiCF_3SO_3$. This polymer/salt combination has been shown to offer good electrochemical stability as well as promising ionic conductivity.[5]

Experimental Section

The source of PEO was the Aldrich Chemical Co. and had a molecular weight of 5×10^6. The $LiBF_4$ used was supplied and analyzed by Lithium Corp. of America showing 0.03% water content. This was additionally dried at 50 °C under vacuum prior to use. $LiCF_3SO_3$ was prepared by reaction of Li_2CO_3 and CF_3SO_3H (trifluoromethanesulfonic acid) in water. The product was dried by warming under a flow of dry nitrogen and recrystallized from an acetonitrile/toluene mixture. The final product was dried in vacuum at 110 °C. The IR spectrum was essentially identical with that of commercial material. All operations performed by using the polymer and salt were done in a dry, inert atmosphere to eliminate water contamination which has been shown to have a significant effect on conductivity measurements.[6] The solids were weighed in a drybox and mixed together with distilled acetonitrile (approximately 1 g of polymer to 50 mL of solvent). Mixtures were stirred in the drybox for ~36 h. Acetonitrile was distilled from anhydrous potassium carbonate and transferred under dry nitrogen to the glovebox before use. Mixtures of (moles of PEO monomer):(moles of Li salt) were prepared ranging from 2:1 to 40:1 for $LiBF_4$ and 25:1 to 1:1 for $LiCF_3SO_3$. Films of the complexes were cast, on a ~500-mg scale on a PTFE plate mold, by permitting the solvent to evaporate in the glovebox at room temperature for 2 days. IR monitoring for residual solvent or H_2O in the films was negative after this time period.

A Du Pont 1090 thermal analyzer was used to perform calorimetry. Samples were prepared in the drybox by cutting pieces of the film into small squares to fit into a hermetically sealed aluminum pan. The temperature scale was calibrated by using a Na standard. Transition temperatures were specified by the

0024-9297/88/2221-0654$01.50/0